Chinese Journal of
POLYMER SCIENCE

RESEARCH ARTICLE

https://doi.org/10.1007/s10118-024-3121-9
Chinese J. Polym. Sci. **2024**, *42*, 751–765

Investigation on UV-curing Reprocessable Thermosets Bearing Hindered Urea Bonds and Their Composites with Modified Zinc Oxide Nanoparticles

Jun-Hao Zhou and Li-Ming Tang*

Key Laboratory of Advanced Materials of Ministry of Education of China, Department of Chemical Engineering, Tsinghua University, Beijing 100084, China

Electronic Supplementary Information

Abstract In this study, a series of hindered urea bond (HUB) containing polyurethane-urea methacrylate prepolymers and a none HUB containing polyurethane methacrylate prepolymer were prepared using isobornyl methacrylate as the reactive diluent *via* one-pot procedure. The prepolymers were characterized fully by various techniques. Then, their thermosets were fabricated *via* UV curing in presence of a photo initiator, and their mechanical property and thermal behavior were investigated and compared. Different from the none HUB containing thermoset, the HUB containing thermosets (defined as PUT) could be recycled and reprocessed by hot press under relatively mild conditions with high recovery ratio of mechanical property. Furthermore, zinc oxide (ZnO) nanoparticles were modified with 3-(trimethoxysilyl) propyl methacrylate and the modified ZnO (defined as ZnO-TPM) was dispersed and polymerized into PUT matrix to prepare their nanocomposites. The influence of ZnO-TPM on the mechanical performance of the composites was evaluated, which indicated that the Young's modulus and tensile strength increased gradually to the maximum values at ZnO-TPM content of 1 wt% and then decreased. The composites also displayed good reprocessability with improved recovery ratio compared to the pure PUT sample. In addition, the composite materials exhibited strong UV absorption capacity, implying their potential application in the circumstance where UV-shielding was required.

Keywords Polyurethane-urea methacrylate; Hindered urea bond; ZnO nanoparticles; Reprocessing; UV curing

Citation: Zhou, J. H.; Tang, L. M. Investigation on UV-curing reprocessable thermosets bearing hindered urea bonds and their composites with modified zinc oxide nanoparticles. *Chinese J. Polym. Sci*. **2024**, *42*, 751–765.

INTRODUCTION

The omnipresent thermosets (or crosslinked polymers), accounting for 15%–20% of global polymer production,[1] have many applications in various areas, like coatings, electronic packaging, adhesives,[2,3] *etc*. The conventional thermosetting plastics possess permanent and irreversible cross-linked networks built by robust covalent bonds. That implies thermosets create increased thermo stability, solvent resistance and mechanical properties than do thermoplastics. Furthermore, they are not susceptible to creep. As a result, resistance to ambient damage by thermal and chemical impulses makes them very suitable for use in structural and protective applications, such as aerospace materials and wind turbines.[4] Unfortunately, thermosetting polymer cannot be recycled due to being unable to be reprocessed by heat or solvents.[5] The non-recyclability of thermosets means economic loss, waste of natural resource and environmental pollution, which runs counter to the concept of sustainable development and environmental protection.

* Corresponding author, E-mail: tanglm@tsinghua.edu.cn

Received January 12, 2024; Accepted March 6, 2024; Published online April 15, 2024

Dynamic covalent bond (DCB) is the key to solve the above problems. It can be reorganized that under external stimuli such as heat or light, achieving the equilibrium between the associated and dissociated states. In comparison to non-covalent interactions, nevertheless, dynamic covalent reactions often require catalyst and harsh stimulus (*e.g.*, high temperature) to complete the equilibrium in a certain timescale because its kinetics are slower.[6,7] On the other hand, the slower kinetics establishes a more stable thermodynamic equilibrium. The recent literature examples utilizing DCBs to recycle, remold or reprocess thermosets include olefin metathesis,[8] transesterification,[9] disulfide metathesis,[10] dynamic B—O bonds,[11] alkoxyamine chemistry,[12] transalkylation,[13] imine bonds,[14] *etc*. However, these dynamic covalent reactions are restricted to the availability of commodity raw materials and usually need to be conducted under demanding conditions, such as high temperature or catalyst, which severely limits their usage scenarios.

What's exciting is that hindered urea bond (HUB), a new kind of DCBs, can be dissociated into isocyanate and hindered amine that has a bulky alkyl group like *tert*-butylamine attached to the nitrogen atom under mild and catalyst-free conditions.[15–17] Many studies demonstrated that HUB can

provide crosslinked polymer with self-healing, recyclability and reprocessability *via* hot-pressing. Zhang *et al*. developed a new class of poly(urea-urethane) thermosets with dynamic HUB, which was synthesized by curing 2-(*tert*-butylamino)ethanol (TBAE) and hexamethylene diisocyanate trimer (THDI).[18] That thermoset had comparable mechanical properties and solvent resistance to conventional thermosets, but showed malleability under mild heating without additional catalyst. Zhu *et al*. designed novel recyclable and reprintable castor oil based photopolymers for digital light processing 3D printing *via* HUBs, the printed objects could be recycled in 4 h at 90 °C or 2 h at 100 °C without any catalysts or solvents.[15] According to the work of Fu's group,[19] implanting HUB crosslinks into poly(methyl methacrylate) (PMMA) networks, with excellent solvent and high temperature creep resistance obtained, could substantially improve Young's modulus, tensile strength, strain at break, and toughness compared to those of thermoplastic PMMA.

In addition, some literatures have researched the composites with HUB-based organic matrix and nano filler, and the latter can give the composites some new features. For instance, Ren *et al*. designed a series of waterborne polyurethane urea composite coatings with polydopamine (PDA) modified carbon nanotubes incorporation, the composite coating showed increased electrical conductivity and corrosion resistance.[20] Lu *et al*. fabricated the dual functional wearable devices using reprocessable polyurea with HUBs polymer substrate and silver nanowires (AgNWs). The as-obtained electrodes are endowed with both electrical heating capability and strain sensing functionality.[21] Zhou *et al*. designed a kind of dynamic cross-linked polyurea/PDA (DCPU/PDA) nanocomposites *via* photoinitiated copolymerization, and that nanocomposites are imparted with enhanced thermomechanical and remotely photoresponsive self-healing properties as well as excellent photothermal effects.[22]

These aforementioned studies demonstrated that the incorporation of nanofiller will not deprive those materials containing HUBs of the self-healing capability or reprocessability. It will rather make the composites having distinguished functionalities. The formed nanocomposite, where inorganic nanoscale particles are incorporated into polymer matrix, can exhibit many improved conductive, electric, thermal and mechanical properties.[23–26] With many excellent characteristics, polyurethane (PU) has been used for many applications, such as coatings, paints, adhesives, biomaterials and foams. In addition, its properties and applicability can be further improved by adding zinc oxide (ZnO) nanoparticles[27] into the polymer matrix. ZnO nanoparticles, a kind of commonly used inorganic filler, have many unique properties and draws wide attention in the fields of dentistry,[28] photocatalysts,[29] water decontaminating agent,[30] sensor,[31] piezoelectric materials,[32] UV-radiation protection,[33] *etc*. Some equipment or commodities (like lipids, flavors, vitamins, and pigments) may be vulnerable to UV radiation and prone to undergo degradation reactions.[34] Other organic materials, such as plastics, polymers, pigments, wood and so on, would occur discoloration, yellowing, darkening and loss of mechanical properties, *etc*., under the action of UV light.[35] Therefore, UV-protection coating/film originated from PU or other materials is often used. The incorporation of ZnO nanoparticles into the coatings can easily achieve UV-shielding in a low-cost and efficient way.

Herein, we report a kind of reprocessable polyurethane-urea methacrylate crosslinked polymers containing HUB motifs (denoted as PUT) fabricated *via* UV curing process. In order to make their mechanical properties able to be tuned over a wide range and suitable for different application requirements (like tough plastic, protective coating, adhesive, and soft elastomers), a series of PUT prepolymers with different chain lengths were synthesized *via* one-pot synthesis strategy. In addition, a conventional polyurethane methacrylate thermoset (PUH)[36] as a counterpart was synthesized so that dynamic dissociation of HUB could be explored in more detail. Moreover, modified ZnO nanoparticles were incorporated into PUT matrix to obtain PUT-based nanocomposites. The influence of nano ZnO on the mechanical performance, reprocessability, thermal stability of PUT-based composites was investigated at length. These nanocomposites also have potential applications in packaging, protective coating, *etc*., thanks to the strong UV-shielding property of ZnO. That means these UV-protection composites can meantime possess reprocessability, reducing the use of traditional fossil fuels.

EXPERIMENTAL

Materials

Poly(propylene glycol) (PPG, M_n=1000 g/mol) was supplied by Adams Reagent Co., Ltd., (Shanghai, China). Isophorone diisocyanate (IPDI; 99%) and ethyl alcohol (99.5%) were obtained from Shanghai Merrill Chemical Technology Co., Ltd., (Shanghai, China). 2-Hydroxypropyl methacrylate (HPMA, 97%) was supplied from Tianjin Zancheng Scientific Co., Ltd. Isobornyl methacrylate (IBOMA, 98%) was purchased from Shanghai Maclean Biochemical Technology Co., Ltd., (Shanghai, China). 2-(*Tert*-butylamino)ethyl methacrylate (TBEM, 99%) was obtained from Anhui Zesheng Technology Co., Ltd. Di-*n*-butyltin dilaurate (DBTDL; chemically pure) was purchased from Sinopharm Chemical Reagent Co., Ltd. (Shanghai, China). Hydroquinone (HQ, analytically pure) was obtained from Beijing Xudong Chemical Plant (Beijing, China). 2-Hydroxy-2-methyl-1-phenyl-propan-1-one (PI 1173, 99%) was purchased from Shanghai Yinchang New Materials Co., Ltd., (Shanghai, China). ZnO nanoparticles (30–80 nm, purity: 99 wt%) was procured from Nanjing Xianfeng Nanomaterial Technology Co., Ltd. 3-(Trimethoxysilyl) propyl methacrylate (TPM, 98%) was purchased from Shanghai Bide Medical Technology Co., Ltd., (Shanghai, China). PPG was pretreated by vacuum drying at 100 °C overnight, and HPMA was dried with anhydrous calcium chloride overnight before use. The other reagents were used as received without further purification.

Preparation of UV Curable Resin

The UV curable resin was prepared *via* one-pot synthesis method without extra solvent and purification process. Table 1 lists the feeding formula for preparing prepolymer resins. Herein, the synthesis process for the PUH prepolymer has been described in detail in our previous work,[36] except that the feeding formula were slightly adjusted. As for the PUT prepolymers,

Table 1 Feeding formula for UV curing prepolymer resins.

Sample [a]	PPG (g, mmol)	IPDI (g, mmol)	TBEM/HPMA (g, mmol)	IBOMA [b] (g)	HQ (mg)	DBTDL (g)	PI 1173 (g)
PUT1	13.175 13.175	4.387 19.763	2.437 13.175	5	12.5	0.04	0.75
PUT2	11.025 11.025	4.895 22.051	4.079 22.051	5	12.5	0.04	0.75
PUT3	9.479 9.479	5.261 23.697	5.261 28.436	5	12.5	0.04	0.75
PUH	11.547 11.547	5.127 23.095	3.326 23.095	5	12.5	0.04	0.75

[a] The molar ratios of PPG:IPDI:TBEM (or HPMA for PUH), which reacted to produce a prepolymer, were 2:3:2, 1:2:2, 2:5:6 for PUT1, PUT2 (and PUH), PUT3 respectively. The molar ratios of —NCO group to the sum of —OH and —NH were 1:1 for all samples; [b] The mass ratio of IBOMA to prepolymer was fixed at 1:4.

the two-step preparation procedures were similar to that of the PUH prepolymer. Briefly, taking PUT1 for example, PPG (13.175 g) and IPDI (4.387 g) were firstly added into a round-bottomed flask. The reactants with DBTDL (0.04 g) as catalyst, were mechanically stirred in oil bath at 70 °C for 2 h. Next, the reaction temperature subsequently was lowered to 50 °C, HQ inhibitor (12.5 mg) and IBOMA diluent (5 g, reducing viscosity) were charged into the flask, and TBEM (2.437 g) was added dropwise to the flask and reacted for additional 2 h. After that, the resin was cooled to room temperature, and PI 1173 (0.75 g) was added. After thoroughly mixed and high-speed centrifugation, the UV curing prepolymer resin of PUT1 was obtained. The UV curable resins of PUT2 and PUT3 were fabricated in the same way.

Modification of ZnO Nanoparticles

ZnO nanoparticles (2 g) was added to a sealed vial with 30 mL of ethyl alcohol and water mixed solvent (9:1, *V*:*V*). The ZnO nanoparticles were magnetically stirred and ultrasonically dispersed for 1 h. Then, 0.16 g of TPM was dropped to the vial. After that, the ZnO suspension was transferred into a 100 mL round bottomed flask and refluxed under magnetic stirring for 3 h at 70 °C. White precipitate was produced after high-speed centrifugation at 8000 r/min for 10 min. The white precipitate was ultrasonically dispersed into 30 mL of absolute ethyl alcohol and recentrifuged at 8000 r/min for 10 min to separate the white precipitate. Repeating this procedure for at least three times to remove impurity. The modified ZnO nanoparticles, denoted by ZnO-TPM afterwards, was obtained after vacuum drying at 60 °C for 24 h.

Preparation of Neat Organic Cured Materials

Both neat PUT and PUH crosslinked materials were obtained *via* UV curing. After carefully pouring the curable resins into a rectangular Teflon mold or other substrates, irradiate the resin for 10 min using mercury lamp (400 W, 365 nm). The distance between mercury lamp and the resin was fixed at 15 cm. Then pure crosslinked materials were obtained and took out for subsequent experiment.

Preparation of PUT-based Composites

PUT2 resin was chosen to fabricate the composite containing different amounts of ZnO-TPM (0.2 wt%, 0.5 wt%, 1 wt% and 2wt% of PUT2, respectively). Firstly, ZnO-TPM nanoparticles and liquid resin were fully mixed mechanically, to make ZnO-TPM dispersed well. The subsequent UV curing procedure was consistent with that of pure organic resins. The corresponding composites were called as PUT2-ZnO*x*. The subscript numeral *x* within "PUT2-ZnO*x*" represented the weight percentage of ZnO-TPM compared to PUT2 resin.

Characterization

Gel permeation chromatography (GPC), Proton nuclear magnetic resonance (^{1}H-NMR), the swelling degree, Shore hardness, adhesion grade, flexibility of crosslinked materials, and the viscosity of liquid resin (full formula) were tested according to our previous work.[36]

Fourier transform infrared (FTIR) spectrum was conducted by infrared spectrophotometer (IR Tracer-100, SHIMADZU Ltd., Kyoto, Japan) in the scan range of 400-4000 cm^{-1} with resolution of 2 cm^{-1}. Liquid resin was recorded by using KBr pellet; the cured samples were recorded by Attenuated Total Reflection (ATR). A thin PUT2 film was used to perform the in-situ temperature dependent IR measurement.

Morphology of the ZnO nanoparticles before and after modification was obtained with a transmission electron microscope (TEM, JEM2010) with an accelerating voltage of 80 kV.

The PUT crosslinked samples were cut into small pieces and soaked into *N*-methylpyrrolidin-2-one (NMP) at room temperature for 30 days. They were then vacuum-dried at 50 °C to a constant weight. The gel content (*G*) of PUT was obtained by Eq. (1):

$$G = \frac{m}{m_0} \tag{1}$$

where m and m_0 are the mass of crosslinked samples after and before soaking into NMP.

The mechanical property of the pure organic cured materials and the composites were determined by tensile test. The films were cut into dumbbell-shaped specimens with the width and thickness of 8 and 1.2 mm, respectively. The gauge length between the two mechanical grips was 30 mm. These specimens were then subjected to tensile test using an Instron 5967 testing machine (Instron Co., Ltd.) at room temperature, and the constant tensile rate was 10 mm/min.

Dynamic thermo-mechanical analysis (DMA) was recorded on a TA Instruments DMA 850 in tensile mode. The size of test samples was 30 mm × 7 mm × 0.5 mm. The temperature ranged from −70 °C to 160 °C with heating rate of 3 °C/min, and the oscillation frequency was 1 Hz. The stress relaxation curves were performed in a "stress relaxation" mode with an iso-strain value set at 1%.

Differential scanning calorimetry (DSC) was measured to study the heat behavior of cured samples *via* the DSC 214 Polyma instrument (NETZSCH) from −100 °C to 140 °C at a heating rate of 10 °C/min under a nitrogen flow.

Thermal gravimetric analysis (TGA) of the cured materials

was performed by a TG 209 thermogravimetric analyzer (NETZSCH Corporation). The tested temperature range was from 35 °C to 750 °C at a heating rate of 10 °C/min, N_2 flow was 20 mL/min.

Scanning electron microscope (SEM, JEOL JSM 7401F) was used to evaluate the morphology of the composites. It was imaged under the accelerating voltage of 3 kV after gold plating.

The UV shield effect of composite cured films was researched by using a UV-3200 spectrophotometer (Mapada, Shanghai, China). The absorbance was scanned in the range of 200–800 nm.

Recycling Experiment

The cured samples were firstly cut into small pieces and put into a mold with the size of 100 mm × 100 mm × 1.2 mm, then hot pressed at 120 °C under 15 MPa for 15 min (The hot-pressing condition for PUT1 sample: 100 °C under 10 MPa for 10 min). After that, the thermocompressor was water cooled to about 40 °C and the obtained sheets were taken out from the machine. The sheet samples were similarly cut into dumbbell-shaped specimens for mechanical testing afterwards. We define these samples that were derived from the original sample *via* hot pressing as the first recycled reprocessing (1R) samples. In a similar fashion, the second recycled reprocessing (2R) samples could be produced after the 1R samples were cut into small pieces and hot pressed again. The 2R samples were subjected to the same procedure to obtain the third recycled reprocessing (3R) samples.

RESULTS AND DISCUSSION

Synthesis and Characterization of the Prepolymers

In this work, UV curable prepolymers were fabricated by a one-pot two-step process. Taking PUT2 and PUH as examples, excessive IPDI was firstly reacted with PPG to form an isocyanate-terminated polyurethane that was then end-capped by methacrylate containing reactants, TBEM or HPMA, thus forming the bifunctional polyurethane-urea (or polyurethane) methacrylate prepolymers with methacrylate groups on both ends using IBOMA as the diluent, as shown in Scheme 1 (the preparation of PUT1 and PUT3 prepolymers are shown in Scheme S1 in the electronic supplementary information, ESI). Upon incorporation of photoinitiator, the solvent-free UV curing resins were finally obtained, then the corresponding crosslinked polymers were fabricated after UV curing. The synthesis and characterization results of PUH prepolymer using HPMA as the end-capping agent, have been described in our previous work[36] and not explained here. As for the synthesis of PUT prepolymer, TBEM with both methacrylate group and bulky amine (*i.e.*, *tert*-butyl amine), was used as the end-capping agent to form HUB containing prepolymers as PUT series (including PUT1, PUT2, and PUT3, see Table 1). Upon UV irradiation, the photoinitiator was disrupted to generate free radicals, which subsequently initiated free-radical crosslinking copolymerization of the prepolymer and IBOMA, thus forming the crosslinked polymers. Owing to the HUB motif, the PUT series crosslinked polymers could be endowed with the capability of being reprocessed repeatedly. Without HUB motif, the conventional polyurethane prepolymer PUH based crosslinked polymer could serve as a counterpart to help investigating the dynamicity and dissociation of HUB motif.

By adjusting the feeding ratio of the raw materials, the prepolymers would have different structure and component, giving rise to crosslinked polymers with diverse performances to satisfy the specific application scenarios. From Table 1, the molar ratios of PPG:IPDI:TBEM are 2:3:2, 1:2:2 and 2:5:6 for PUT1, PUT2 and PUT3, respectively. Ideally, PUT1 prepolymer has the molecular structure of TIPIPIT where T, I, P denote the segments of TBEM, IPDI and PPG, respectively. In the same manner, PUT2 prepolymer corresponds to TIPIT, a shorter molecular chain. While PUT3 prepolymer is constituted of both TIPIT and TIT at their molar ratio of 2:1. Simultaneously,

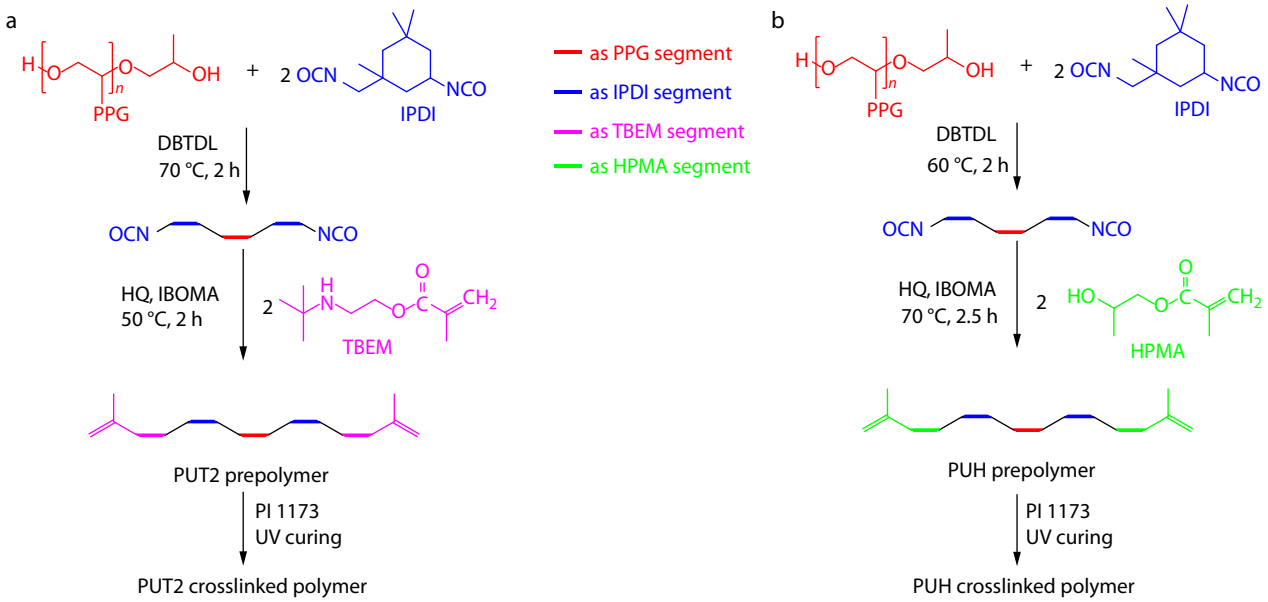

Scheme 1 Schematic diagram for the preparation of (a) PUT2 and (b) PUH crosslinked polymers.

the conventional prepolymer PUH has the similar structure to that of PUT2, namely HIPIH, where H denotes the segment of HPMA. Therefore, the average molecular length became shorter and shorter from PUT1 to PUT3. It is foreseeable that the cured crosslinked network of PUT1 would correspond to the smallest crosslinking density, PUT3 correspond to the largest one, while PUT2 and PUH are medium, which is just opposite to the molecular length of the prepolymers. So that the performance of the cured materials can be modulated over a considerable range and the reversible chemistry of HUB could be elucidated more deeply by contrasting the two systems of PUT2 and PUH.

The GPC curves and the corresponding number-average molecular weight (M_n) of those prepolymers are shown in Fig. 1(a). The GPC curve of PUT1 prepolymer, with the shortest retention time (8.9 min) and largest M_n, presents a unimodal distribution. As expected, PUT3 prepolymer displays a typical bimodal molecular weight distribution. The peak with a short retention time (~9.2 min) corresponds to the TIPIT structure, and the peak with a long retention time (~9.9 min) corresponds to the TIT structure. In ideal conditions, the GPC curves of PUT2 and PUH prepolymers, whose structures and M_n are similar, should exhibit a unimodal distribution with the peak at about 9.2 min. Actually, both PUT2 and PUH prepolymers exhibit an additional small peak at 9.9 min. That is because little amount of unreacted IPDI, left over after the first step reaction for preparing isocyanate-terminated polyurethane, would be directly capped by TBEM or HPMA in the subsequent reaction unavoidably.[36] The FTIR spectra of PUT2 prepolymer (before curing) and PUT2 cured sample (after curing) are shown in Fig. 1(b). It can be observed that the —N=C=O stretching vibration band (2260 cm^{-1}) entirely disappears from the FTIR spectrum of PUT2 prepolymer, which shows the synthesis reaction of the prepolymer is complete. The characteristic bands at 1660 and 1716 cm^{-1} are attributed to C=O stretching vibration of urea (—N—CO—N) and carbamate (—N—CO—O) groups, respectively, while the broad band at 3405 cm^{-1} can be attributed to N—H stretching vibration of both urea (—N—CO—N) and carbamate (—N—CO—O) groups. The characteristic bands at 1638 and 815 cm^{-1} are attributed to C=C stretching vibration and bending vibration, respectively. Furthermore, the characteristic bands at 1638 and 815 cm^{-1} disappear after the prepolymer being cured, indicating that the conversion of methacrylate groups and curing content are fairly high. Moreover, the ^{1}H-NMR spectrum of PUT2 prepolymer, as a representative, is shown in Fig. S1 (in ESI). It is noticed that all the typical hydrogen protons in the molecule of PUT prepolymer could be identified in the spectrum. The above results confirmed that the polyurethane-urea methacrylate prepolymer had the desired molecular structure.

Dynamic Reversibility of HUB

The dynamic chemistry of HUB at elevated temperature could be verified by temperature-dependent FTIR method. As shown in Fig. 2(a), the characteristic band of —N=C=O at around 2265 cm^{-1} showed up and intensified with increasing the temperature whereas it did not exist at room temperature (25 °C). In addition, the band of —N—H of carbamate group at around 3400 cm^{-1} became weakened gradually. That may be ascribed to the dissociation of both HUBs and hydrogen bonds.[15] The schematic diagram of HUB dissociation is depicted by Fig. 2(b). These results reveal that HUBs underwent enhanced dissociation at elevated temperatures and maintained the stable associated state at low temperature.

Theoretically speaking, due to its permanent three-dimensional covalent network, the crosslinked polymer prepared by UV curing did not have the ability of being reprocessed by heating or solvent. The situation would be different if dynamic covalent bond, *e.g.*, HUB, is introduced to the crosslinked network. In order to verify that HUB containing crosslinked polymer could be dissolved and recycled using solvent and heating, the cured samples of PUT1-PUT3 and control sample PUH were soaked in NMP and heated at 100 °C. Obvious swelling would occur in the samples of PUT1-PUT3 after 7 h (Fig. 3a). As the time prolonged, the PUT samples were dissolved absolutely at different time. It took more time to be dissolved from PUT1 to PUT3 samples, corresponding to their gradually increased crosslinking densities. By contrast, the PUH sample, constituted fully by conventional covalent bonds, was insoluble even being heated in NMP for 20 h. This result demonstrated that HUB could dissociate under the actions of both heating and dissolving. Furthermore, we stud-

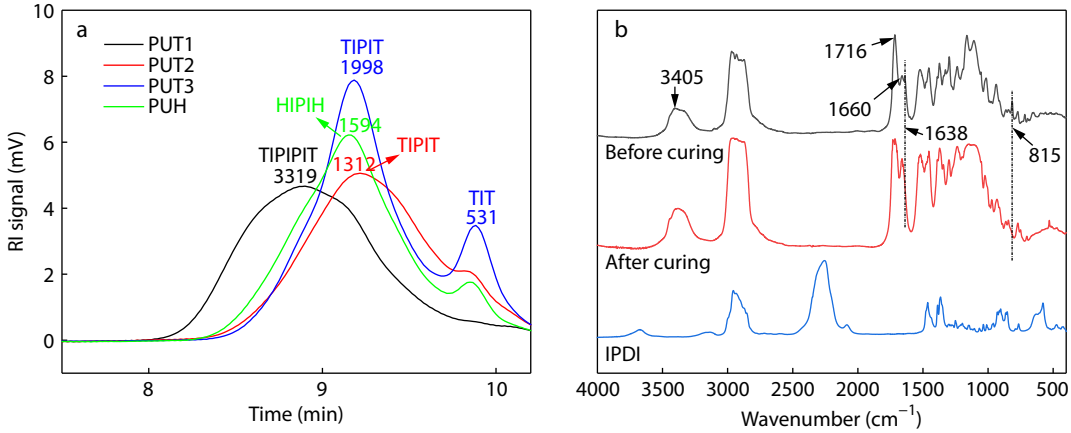

Fig. 1 (a) GPC curves of PUT and PUH prepolymers with the corresponding structure and number average molar mass (M_n) indicated in the curves; (b) FTIR spectra of PUT2 resin before and after curing.

https://doi.org/10.1007/s10118-024-3121-9

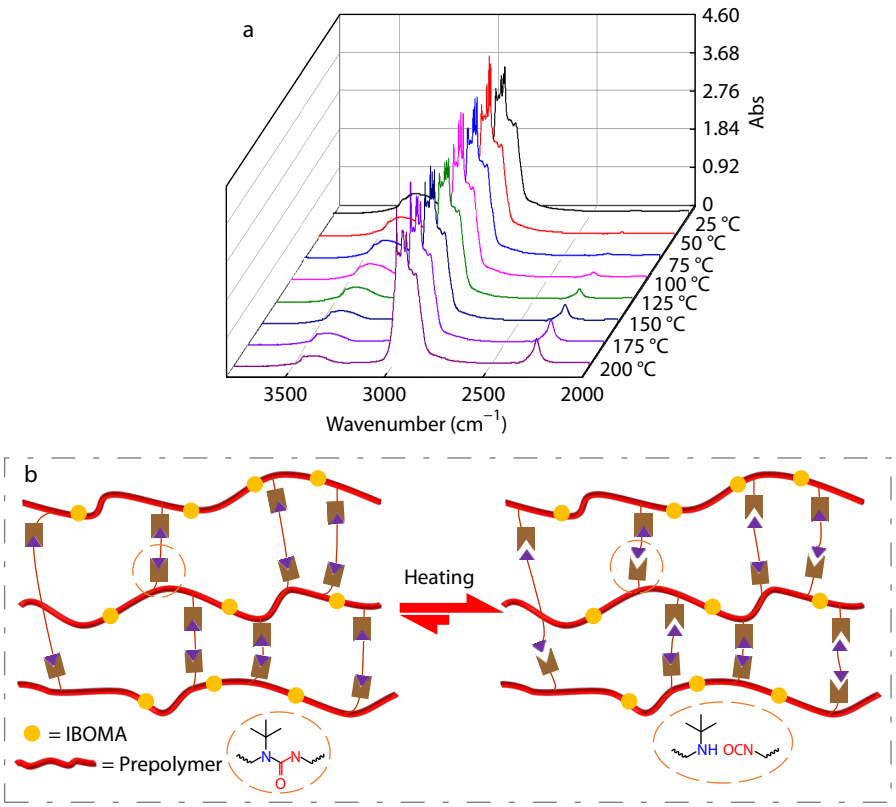

Fig. 2 (a) Temperature-dependent FTIR spectra of PUT2 cured film; (b) Schematic diagram of HUB dissociation under thermal stimulus.

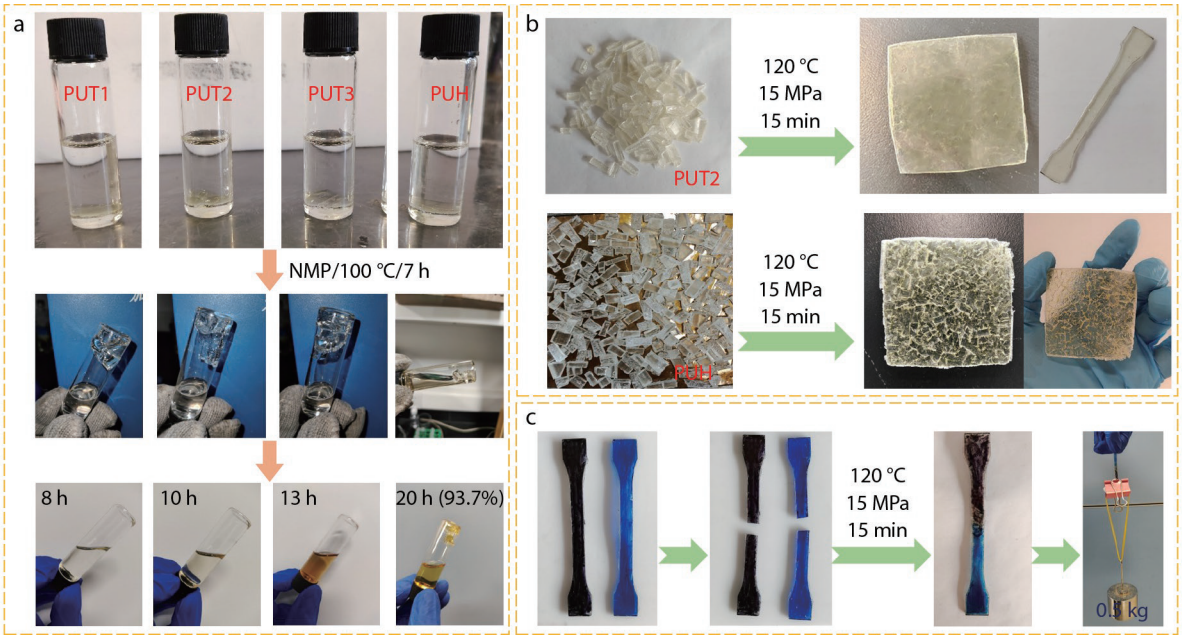

Fig. 3 (a) Solubility of cured samples: obvious swelling occurred in PUT1-PUT3 samples after soaked in NMP at 100 °C for 7 h, while PUH changed slightly (middle row); the PUT1, PUT2 and PUT3 samples were dissolved absolutely at 8 h, 10 h and 13 h, respectively; the residual mass of PUH (i.e., gel content) was 93.7% (lower row); (b) comparison of PUT2 and PUH samples after being hot pressed; (c) PUT2 specimen could be welded and bear the weight of 0.5 kg for a long period.

ied the solubility of PUT2 sample in multiple solvents (including water, ethanol, acetone, toluene, and NMP) at room temperature. PUT2 sample underwent evident swelling in organic solvent while the swelling was relatively minor in water after 6 days (Fig. S2 in ESI). After 30 days, not much change had occurred in swelling and appearance of the sample, similar to that of PUH sample. So PUT2 sample always maintained an integrated one in various solvents if no heating was applied. It

reveals that although the HUB had the characteristic of dynamic reversibility, HUB containing polymer still possessed the stability of conventional thermosets at room temperature. The swelling and residual mass of the PUT2 and PUH samples after being soaked in different solvents are summarized in Fig. S3 (in ESI). As expected, the swelling and residual mass of PUT2 sample are respectively a little larger and smaller than PUH sample. The gel content of PUT1-PUT3 samples (soaked in NMP for 30 days) was determined to be 87.5%, 90.2%, and 91.5%, respectively. The gel content showed positive correlation with the crosslinking density of these samples, and such high values indicated that PUT thermosets could maintain stability if only being treated with solvent.

At the recycling experiment, small pieces of PUT2 sample could be processed into intact plastic block by hot pressing while there were many defects in the PUH control specimen (Fig. 3b). In fact, the small pieces of PUH did not fuse at all and apparent remolding marks existed in the sample. From Fig. 3(c), we can see that two broken dog-bone-shaped specimens of PUT2 could be welded into a reborn one that could even bear quite high weight (0.5 kg) without broken. Combined with temperature-dependent FTIR spectra (Fig. 2a), the solubility, reprocessability and weldability of PUT samples, it is demonstrated that HUB could impart the chemical bonds with dynamic reversibility and make crosslinked polymer possessing the properties commonly found in thermoplastics.

The above hot pressing experiments have demonstrated that HUB is able to provide reprocessability to PUT samples. It can be anticipated that those PUT materials might own some degree of self-healing capability, a feature of crucial importance for thermosets in practical application. Scratch-healing test was then conducted to confirm this conjecture. The original PUT and PUH films were firstly scratched by a razor blade on which the width of the scratch was about 100 μm, then they were transferred to an oven at 80 °C for 180 min. The changes in scratches during this period were recorded by an optical microscope (WMP-6508). Although all PUT materials displayed healability to some extent which resulted from dynamic urea exchange reactions, PUT1 film possessed the most wonderful self-healing ability and the scratch on it was no longer discernible but vanished almost completely (Fig. 4). While PUT2 and PUT3 films exhibited somewhat decreased self-healability (PUT2>PUT3) relative to PUT1, the scratches on them were still observed, *i.e.*, not yet fully healed. That result may be attributed to the higher crosslinking density and lower chain mobility in them.[37] As for PUH sample without HUB, the scratch was only slightly diminished probably thanks to the hydrogen bond of carbamate groups, and it can be considered that PUH sample has no self-healability. The reprocessability and self-healability of PUT heralded that the PUT materials have the potentiality to be applied as self-healing protecting coating.

Mechanical Property and Reprocessability of Pure PUT Materials

Tensile tests were performed to further evaluate the mechanical property and reprocessability of PUT materials. The original tensile testing curves are depicted in Fig. 5(a). The Young's modulus (E) increased gradually from 3.81±0.23 MPa of PUT1 sample, to 153.63±8.16 MPa of PUT2 sample, and further to 488.23±27.25 MPa of PUT3 sample. The ultimate tensile strength (σ) exhibits a similar variation trend, which are 1.87±0.15, 7.20±0.43, and 15.53±1.27 MPa for PUT1, PUT2 and PUT3 samples, respectively. The elongation at break (ε) shows a just opposite pattern, those values are 108.12%±7.24%, 73.13%±5.68% and 11.17%±2.11% for PUT1, PUT2 and PUT3 samples, respectively. This result was in line with our expectations and previous work,[36] *i.e.*, the crosslinking density was enlarged and that gave improved mechanical property from PUT1 to PUT3 samples. Furthermore, the increasing content of hard segment especially rigid IPDI moieties and carbamate groups, from PUT1 to PUT3 samples, also enhance the mechanical property. In addition, it is also easy to understand that the two tensile testing curves of PUT2 and PUH samples are rather similar. The E, σ and ε of PUH sample are 122.84±6.72 MPa, 8.00±0.71 MPa and 59.91%±3.84%, respectively. The only difference be-

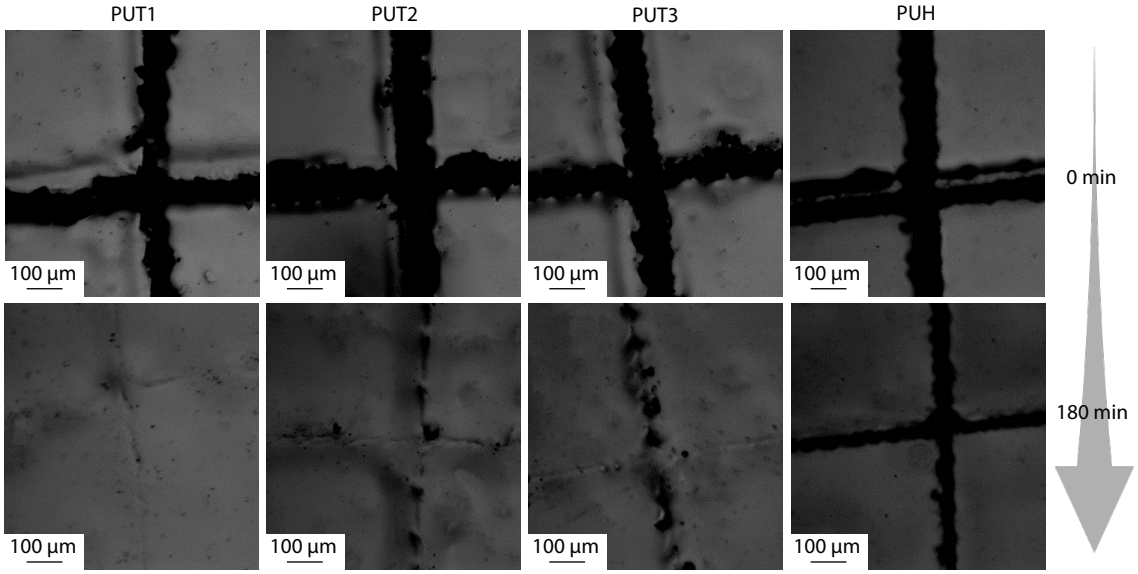

Fig. 4 Scratch-healing process of the cured samples recorded by optical micrographs after being heated at 80 °C for 180 min.

https://doi.org/10.1007/s10118-024-3121-9

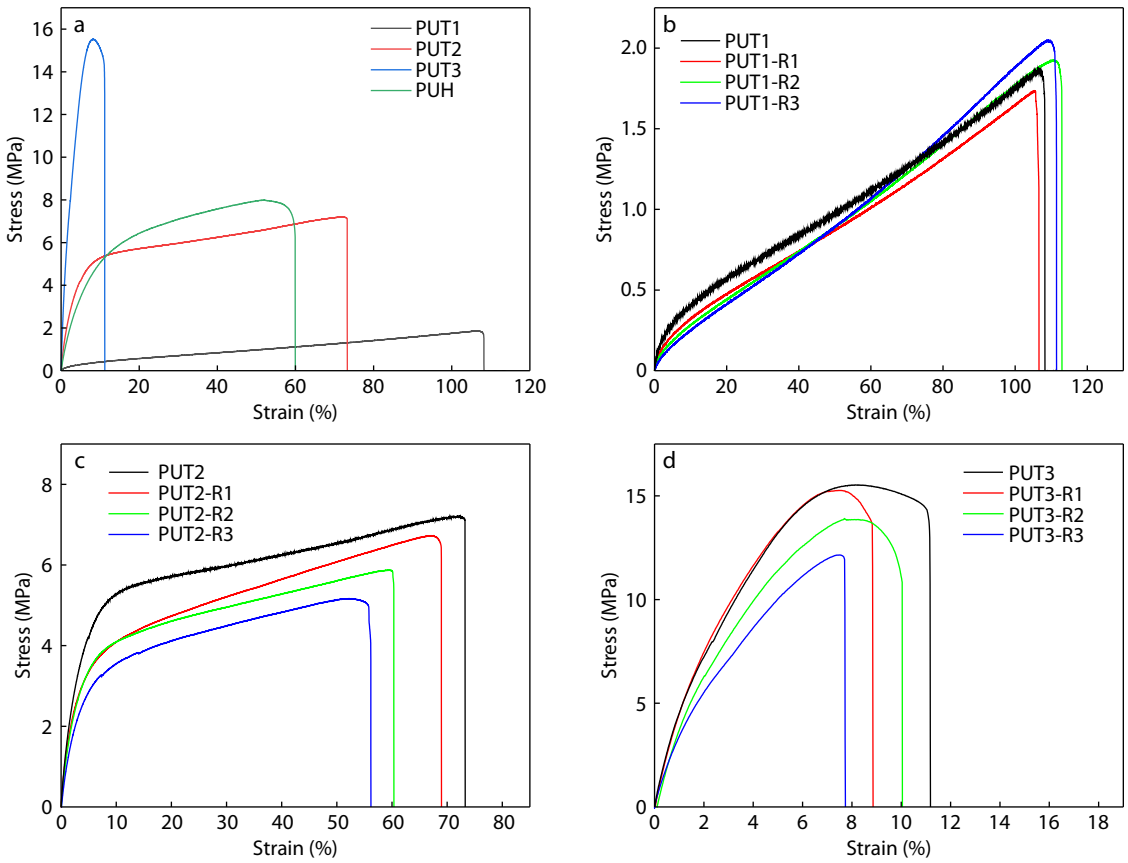

Fig. 5 (a) Original stress-strain curves of PUT1–PUT3 and PUH samples; stress-strain curves of (b) PUT1 sample, (c) PUT2 sample and (d) PUT3 sample after being reprocessed for different time.

tween these two curing systems is the end-capping reagent, TBEM for PUT2 and HPMA for PUH, the structures of both crosslinked networks are naturally similar. Based on the above results, PUT1 sample is just like an elastomer, PUT2 and PUH samples can be regarded as tough plastic, while PUT3 sample belongs to hard plastic. Thus, the mechanical performance of those UV cured crosslinked polymers can be modulated to a wide range by simply adjusting the stoichiometry of the raw materials.

Figs. 5(b)–5(d) show the tensile testing curves of PUT materials before and after reprocessing, with the related parameters listed in Table S1 (in ESI). PUT1 sample, with the lowest mechanical strength and highest ε, could maintained superb recycling stability even after being reprocessed for 3 times, and the tensile testing curves did not exhibit obvious decline in both σ and ε, whose recovery ratios are nearly 100% (Fig. 5b and Table S1 in ESI), reflecting that HUB is an excellent alternative for fabricating processable crosslinked polymer. But for PUT2 and PUT3 samples, their E, σ and ε would decrease a bit after each reprocessing (Table S1 in ESI). After reprocessing for three times, the recovery ratios of σ and ε are lower than 80%. Compared with other studies,[15,18,38,39] those are not fairly ideal values. At the recycling experiments, small pieces of the samples were hot-pressed firstly at the conditions: 120 °C/15 MPa/15 min (except for PUT1: 100 °C/10 MPa/10 min). Then, the samples were water cooled to ~40 °C rapidly, and the resulting sheets were used for tensile tests directly. We conjectured that the stiff PUT2 and PUT3 samples, relative to PUT1 sample, did not have sufficient time to restore to the pristine state at such a limited time interval. Though their mechanical properties would be impaired partly, the recovery ratios of Young's modulus and elongation at break still be maintained to some extent (Table S1 in ESI). In a word, the reprocessing experiment proved that HUB will experience enhanced dissociation under certain conditions and can impart crosslinked polymer with the ability of being recycled. In addition, the Shore hardness of the samples exhibited a similar rule with the mechanical property, which was enhanced from PUT1, PUT2 (PUH) to PUT3 gradually. When the liquid resins were UV cured directly on tin plates, the adhesion grade, flexibility of the resulting coatings are all at the highest level (Table S2 in ESI), which shows that the PUT resins can be served as coatings with favorable mechanical properties. The viscosity of the liquid resins (full formula) is also listed in Table S2 (in ESI).

Through the abovementioned temperature dependent FTIR test, solubility and recycling experiment, it can be confirmed that HUB would experience fast dissociation in response to heat stimulus and produce a thermoset with dynamic crosslinking network that can be recycled through hot press just as thermoplastics. For better understanding the thermomechanical properties of such kind of materials, DMA was utilized to investigate the thermomechanical property with temperature ramping. What needs to be pointed out is

https://doi.org/10.1007/s10118-024-3121-9

that PUT1 sample was prone to fracture at such DMA test condition, so only PUT2, PUT3, and PUH were subjected to DMA analysis. Fig. 6(a) indicates the change of the storage modulus (E') of PUT2, PUT3 and PUH samples as the temperature. At the beginning (<−40 °C), all samples display a stable storage modulus corresponding to the high rigidity. And the E' of PUT2 and PUH samples were very close below 70 °C, just as their tensile testing curves (Fig. 5a). With the increase of temperature, especially in the vicinity of glass transition temperature (T_g), their storage moduli dropped rapidly. The E' of PUH sample reached rubbery plateau and began to level off at above 80 °C. The crosslinking density (v_e) of PUH sample can be estimated by the rubbery modulus according to Eq. (2):[40]

$$v_e = \frac{E'}{3RT} \quad (2)$$

where E' is the storage modulus in the rubbery plateau region, T represents the absolute temperature T_g + 40 °C (in the rubbery plateau region), R is the gas constant 8.314 J·mol^{-1}·K^{-1}. Thus, v_e was calculated as 337.9 mol/m^3. PUH sample accorded well with the kinetic theory of rubber elasticity, whereas PUT sample did not display rubbery plateau which was quite different from PUH sample. The storage modulus of PUT sample dropped continually after T_g, implying that HUB had begun to dissociate and gave rise to bond exchange (at about 80 °C), inducing the promotion of chain mobility, and afterwards the macroscopic flow.[41] The selected temperature 120 °C at recycling experiment is far above the HUB dissociation temperature, and this may explain why HUB makes PUT recovered so efficiently. According to Fig. 6(b), we can find two peaks in the loss factor curves, one is at around −20 °C corresponding to the T_g of soft segment (mainly PPG segment), another at above room temperature ascribed to the T_g of hard segment (mainly hydrogen bond aggregation domain and rigid IBOMA segment). Those values of T_g are listed in Table 2. As was expected, PUT2 and PUH samples had nearly equal T_g's since these two polymers had similar components and structures. PUT3 sample, with higher crosslinking density, displayed a ~20 °C higher T_g of hard segment than PUT2 sample. The loss factor of PUH sample went through continuous declination after T_g, mainly due to the decrease of loss modulus (Fig. S4 in ESI). Different from PUH sample, the loss factors of PUT samples began to rise again at above 110 °C, this is because HUB dissociation made the elasticity weaker meanwhile loss modulus increased leading to viscous deformation occurs progressively (Fig. S4 in ESI).

In addition, stress relaxation experiment was also performed on DMA to investigate the dynamic property of PUT2 sample. The characteristic relaxation time, at the time stress G decreased to 1/e of the initial stress G_0, was reduced owing to faster HUB exchange reaction as the temperature increased

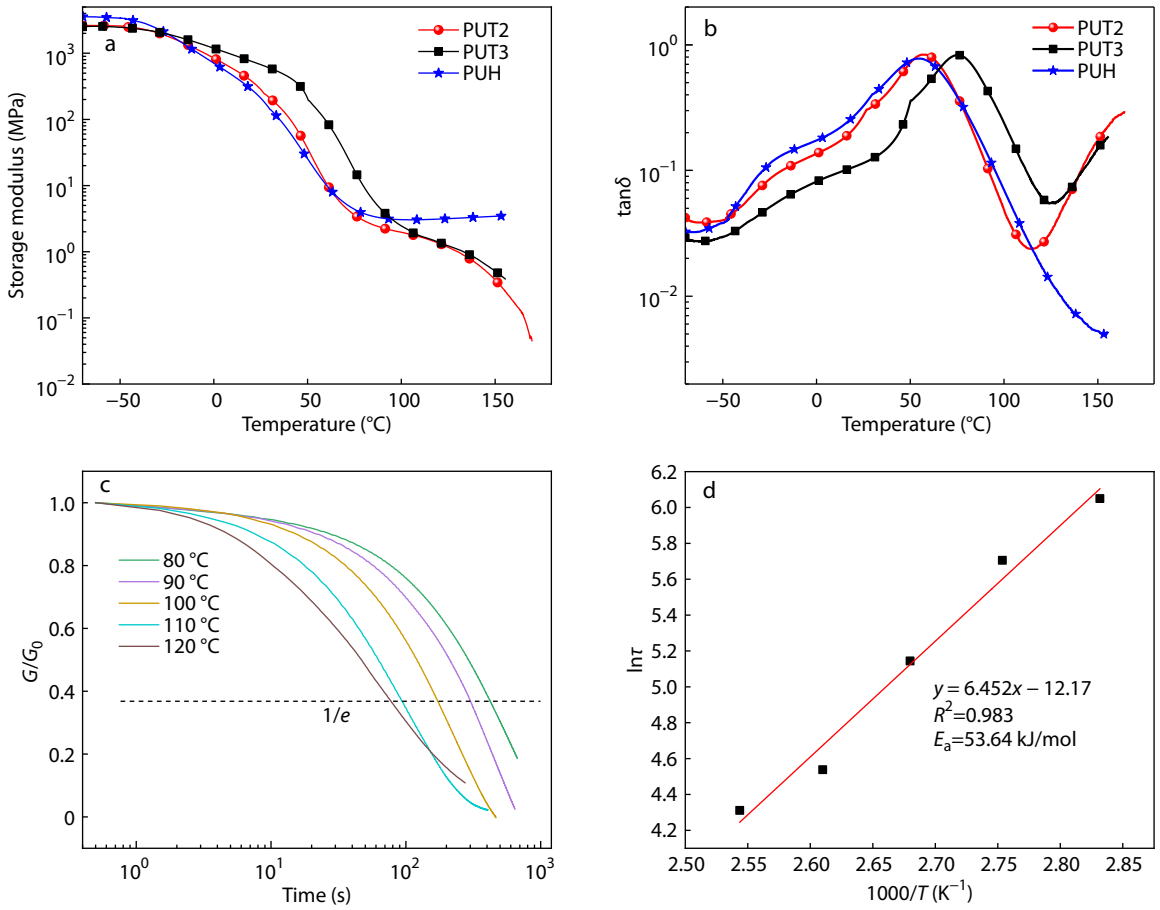

Fig. 6 (a) Storage modulus and (b) loss factor of PUT2, PUT3 and PUH samples versus temperature, (c) stress relaxation analysis results and (d) Arrhenius equation fitting for PUT2 sample.

https://doi.org/10.1007/s10118-024-3121-9

Table 2 Thermal properties of different samples based on DMA, DSC, and TGA results.

Sample	T_g [a] (°C)	T_g [b] (°C)	T_g [c] (°C)	T_i [d] (°C)	T_{max} [e] (°C)
PUT1	–	–	−17.7	246.7	321.8
PUT2	57.2	−20.6	−15.1	241.8	319.3
PUT3	75.4	−20.0	−17.8	202.3	318.1
PUH	54.7	−19.9	−10.4	257.6	329.3

[a] T_g of hard segment by DMA; [b] T_g of soft segment by DMA; [c] T_g of soft segment by DSC; [d] Initial decomposition temperature at 5% weight loss; [e] Maximum degradation temperature.

(Fig. 6c). PUH sample showed in fact the opposite trend, the stress relaxation became slower at higher temperature (Fig. S5 in ESI), proving again PUH was a stable thermoset and no bond exchange occurred within the sample. The activation energy E_a of PUT2 can be calculated by Arrhenius Eq. (3):

$$\tau_T = \tau_0 e^{E_a/RT} \quad (3)$$

Fig. 6(d) presents the fitting result with R^2 at 0.983, indicating the model fits the data well. The calculated E_a is 53.64 kJ/mol, lower than that of some other reprocessable thermosets.[15,16,42] This result is favorable for effective recycling of PUT samples.

Overall speaking, the polymer chains of PUH and PUT, a kind of block polymer, is composed of two different parts. One is called soft segment (like polyether chain) in the elastic state while the other, known as hard segment (including carbamate group, chain extender and crosslinker), is in the glassy or crystallized state at room temperature. The arrangement of alternating hard and soft segments makes polyurethane or polyurethane-urea having very unique properties, *e.g.*, microscopic phase separation with two different T_gs. The T_g of soft segment is usually below room temperature. Due to the presence of a large number of polar groups, *i.e.* carbamate, the hard segment would display a higher T_g. The DMA results, as mentioned above, have demonstrated that the two T_g's coexist in PUT and PUH samples (Table 2). According to the DSC curves of those materials (Fig. S6 in ESI), the four samples all manifested a distinct transition between −10 and −20 °C corresponding to the T_g of soft segment. The T_g of soft segment measured by DSC are also listed in Table 2, and this is not much dissimilar to the test results by DMA. Unfortunately, in the DSC curves, the T_g's of hard segment of all samples did not be observed at around 50–70 °C, suggesting that the hard segments of those materials are insensitivity to thermal effect.

HUB, as is already known, would experience enhanced dissociation and exchange reaction under heating condition. The materials consisting of HUB must possess certain thermal stability so that they can serve as qualified reprocessable thermoset for daily or industrial use. TGA were performed to estimate the thermal stability of PUH and PUT samples. Fig. 7 shows the TGA curves and derivative thermogravimetry (DTG) curves of these samples. The initial decomposition temperature (T_i, 5% weight loss) and maximum degradation temperature are listed in Table 2. From PUT1 to PUT3 samples, the content of HUB moiety increased gradually. The initial decomposition temperature of PUT1 sample was 246.7 °C, while it decreased to 241.8 °C for PUT2 sample, and dramatically further decreased to 202.3 °C for PUT3, meaning that the thermal stability of PUT samples was negatively correlated with HUB content due to its dissociation upon heating. The thermal stability of PUH sample with the T_i at 257.6 °C exceeded apparently that of PUT samples (Fig. 7a and Table 2). The maximum degradation temperature followed similar rule, merely tendency for discrepancy among them was small comparatively. With respect to DTG curves (Fig. 7b), all of the four pyrolysis processes can be divided into three steps, attributed to the degradation of (1) carbamate region (hard segment), (2) thermotolerant polyether chain (soft segment), and (3) the char residue in turn.[36] TGA results revealed that no significant difference was found among PUT and PUH samples, and the PUT materials could still sustain satisfactory thermal stability with their initial decomposition temperature all higher than 200 °C, far above the typical reprocessing temperature (120 °C).

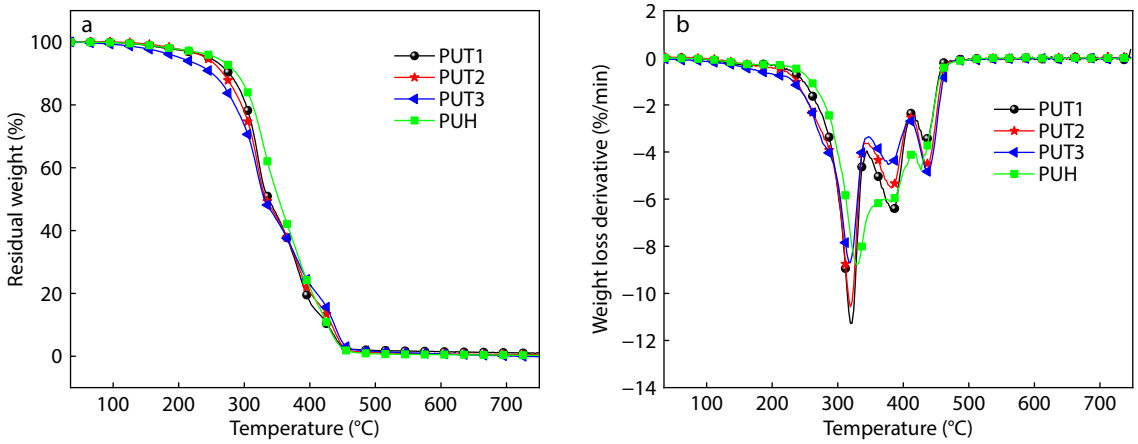

Fig. 7 (a) TGA and (b) DTG curves of PUT1–PUT3 and PUH samples.

https://doi.org/10.1007/s10118-024-3121-9

Synthesis and Characterization of ZnO-TPM and the Composites

Inorganic filler can strengthen the mechanical performance of a composite compared with pure polymer matrix and offer the composite many unique properties which single one of parent constituents does not possess.[43] Hence, this work aims to research the effect of incorporating ZnO nanoparticles to PUT on the mechanical property and reprocessability of the composites. Meanwhile, the strong UV-shielding property of ZnO nanoparticles makes the composite showcase a promising perspective where the composite with reprocessing ability and adjustable performance can serve as UV protection coating under harsh environmental conditions. In order to prevent the agglomeration of ZnO nanoparticles meanwhile enhance the compatibility between ZnO nanoparticles and the polymer matrix, the ZnO nanoparticles were firstly surface modified by silane coupling agent TPM bearing methacrylate group. The hydroxyl groups on the surface of ZnO nanoparticles can react with TPM, so that organic chains with methacrylate group at the chain end were introduced into ZnO nanoparticles, as depicted by Fig. S7(a) (in ESI). After purification, the obtained ZnO-TPM nanoparticles were characterized by FTIR instrument, and the corresponding spectra are shown in Fig. S8 (in ESI). From the spectrum of ZnO-TPM, the broad band at 3450 cm^{-1} is assigned to O—H (hydroxyl group) on the surface of ZnO nanoparticles, the band at around 2950 cm^{-1} corresponds to the characteristic vibration of $-CH_2-$ and $-CH_3-$ of TPM chain. The bands at 1705 and 1631 cm^{-1} belong to C=O and C=C groups of TPM chain, respectively. The strong absorption at 528 cm^{-1} can be assigned to Zn—O bond of ZnO nanoparticles. The bands at 1176 and 1203 cm^{-1} correspond to Si—OH stretching vibration. These results prove the ZnO nanoparticles was modified by TPM successfully.

The TEM images (Fig. S9 in ESI) reveal that serious agglomeration of the pristine ZnO nanoparticles occurred due to strong surface effect; while the ZnO-TPM dispersed more well as separated nanoparticles. Besides, the suspension of ZnO nanoparticles in ethanol (~1 wt%) would precipitate after being stored still overnight, whereas the ZnO-TPM suspension remained good stability (Fig. S10 in ESI). These results prove again that the ZnO nanoparticles were successfully surface modified by TPM. Fig. S7(b) (in ESI) shows the structural schematic diagram of PUT-based composite which was still fabricated *via* UV curing of the mixture of ZnO-TPM and PUT prepolymer resin. In the composite, the ZnO-TPM nanoparticles with methacrylate groups on the surface can participate in crosslinking copolymerization with other components, thus reinforcing the composite.

The morphological structure is of extreme importance because it ultimately affects many physical properties such as the thermal stability and mechanical property of the materials.[44] The morphology of the composites was investigated by SEM to evaluate the dispersion of ZnO-TPM in PUT matrix. Fig. 8 shows the SEM images of the fractured surface of the composites (broken under liquid N_2) with different contents of ZnO-TPM nanoparticles. In comparison with pure PUT matrix corresponding to the Fig. 8(a), white spots, *i.e.*, ZnO-TPM nanoparticles, in the SEM images of the composites (Figs. 8b–8e) are easily observed. And the white spots were getting denser as more ZnO-TPM nanoparticles were used. Overall,

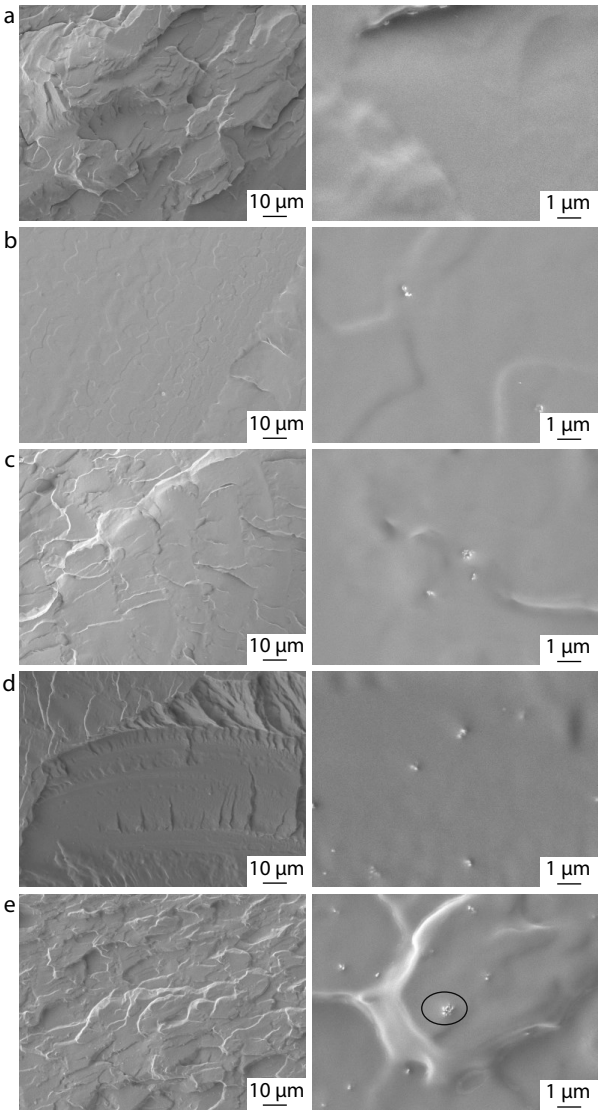

Fig. 8 SEM images of the fractured surfaces of (a) PUT2 sample, (b) PUT2-$ZnO_{0.2}$ sample, (c) PUT2-$ZnO_{0.5}$ sample, (d) PUT2-ZnO_1 sample, and (e) PUT2-ZnO_2 sample. The images on the left and right of each row have a magnification of 1000× and 10000×, respectively.

the nanoparticles could be homogeneously dispersed in the matrix but the agglomeration of nanoparticles may also occur, especially at high content (2 wt%). In this regard, an obvious agglomeration (marked by a black circle) can be noticed according to the right image of Fig. 8(e).

These results demonstrated the ZnO-TPM nanoparticles could be stabilized to achieve a uniform and homogeneous distribution in the composites, suggesting that there is good compatibility between the nanoparticles and the polymer matrix.

Effect of ZnO-TPM on the Composites

The aim of modifying ZnO was to enforce the compatibility and stability of inorganic nanoparticles within the composite. The obtained ZnO-TPM nanoparticles, having methacrylate groups on the surface, could participate in UV curing with other components and act as a part of the cross-linked network. Tensile

https://doi.org/10.1007/s10118-024-3121-9

testing was conducted to inspect the relationship between the mechanical property of the PUT-based composites and the content of ZnO-TPM incorporated, using PUT2 sample (with medium mechanical performance) as the matrix. From the tensile testing curves in Fig. 9(a), the effect of ZnO-TPM content on Young's modulus and tensile strength of the composites is summarized in Fig. 9(b). It can be found that the addition of ZnO-TMP had some influence on the mechanical properties of the composite materials. The original E and σ of PUT2 sample are 153.63±8.16 and 7.20±0.43 MPa, respectively, those values show a gradual upward trend after the addition of ZnO-TPM. Table S3 (in ESI) lists some parameters of the tensile testing curves of the composites. For example, the E and σ of the composite, with 1 wt% ZnO-TPM content, increased to the maximum values of 290.72±20.94 MPa and 8.62±0.68 MPa, respectively. However, in the case of excessive addition of ZnO-TPM, *i.e.*, 2 wt%, the mechanical property might be decreased, with E of 216.28±8.23 MPa and σ of 6.23±0.59 MPa. These results indicated that at the adequate content of ZnO-TPM, the nanoparticles could reinforce the composite, giving rise to the improved mechanical strength. On the flip side, combined with Fig. 8(e), the decrease of the mechanical strength at 2 wt% ZnO-TPM content may be ascribed to the agglomeration of excess nanoparticles in PUT2 matrix and the decreased compatibility of the composites, which would inhibit the strengthening of the mechanical property.[43] Besides, the elongation at break was feebly decreased after the addition of ZnO-TPM in comparison to PUT2 counterpart, probably because of the formation of more rigid crosslinked network.

Then, the reprocessability experiments were performed based on PUT2-ZnO_2 composite to investigate the recyclability of those composites. We found that the composite could still be reprocessed under the typical conditions: 120 °C/15 MPa/15 min, indicating the composites still had good reprocessability. Table S4 (in ESI) lists the relative parameters of the tensile testing curves based on the composites being reprocessed. The E was nearly constant at about 65 MPa after each reprocessing (Fig. 9c), an obvious decline compared to the original PUT2-ZnO_2 (~216 MPa). It's worth noting that the recovery ratios of ε and σ could reach 147.31% and 93.74%, respectively, after the first reprocessing. The recovery ratios of ε and σ still kept high values (127.37% and 86.04%) even after the third reprocessing (Fig. 9d and Table S4 in ESI), which were promoted greatly compared with those (76.78% and 71.81%) of the pure PUT2 sample (Table S1 in ESI).

Thermal decomposition behavior of PUT based composites (Fig. S11 in ESI) did not display much difference for the samples with different contents of ZnO-TPM. DTG curves of all

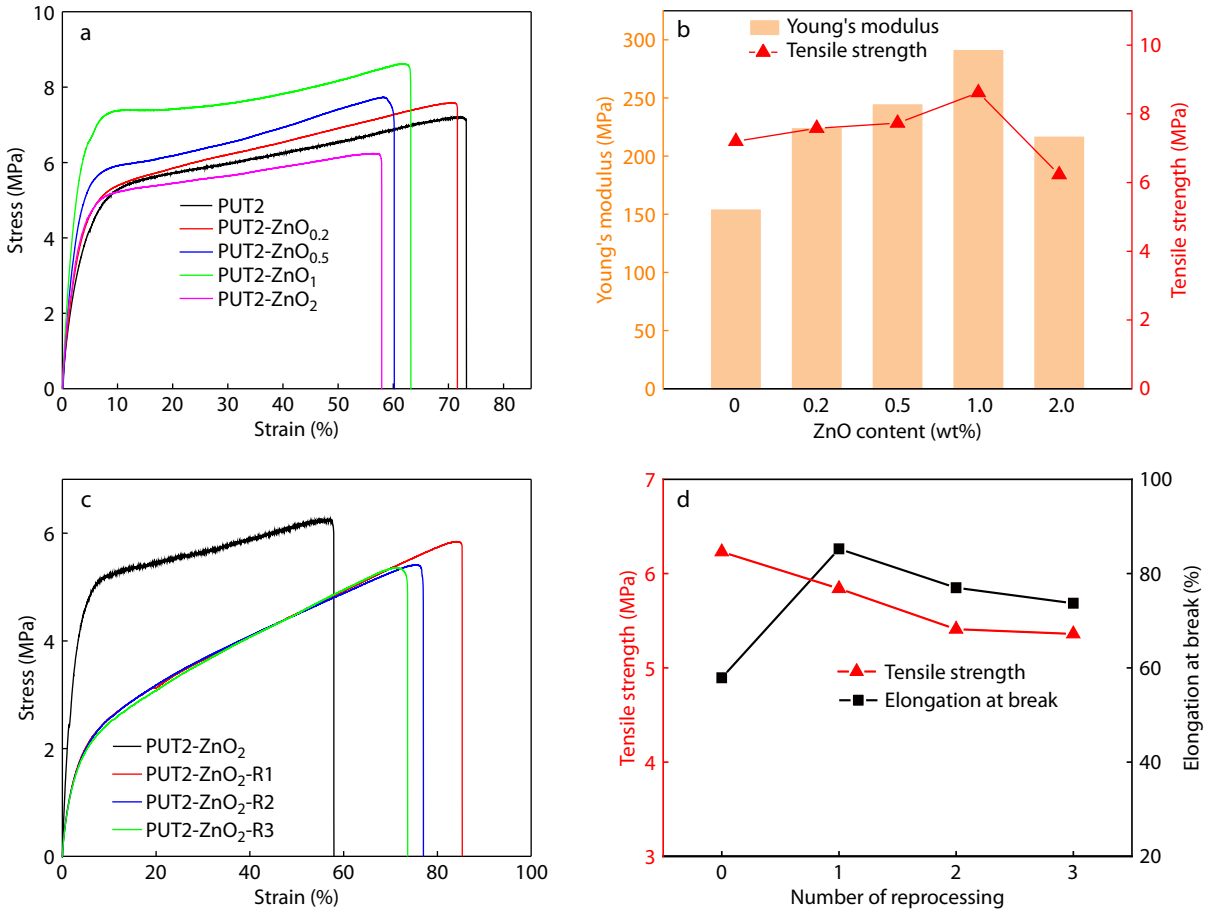

Fig. 9 (a) Stress-strain curves of the composites with different contents of ZnO-TPM; (b) Effect of ZnO-TPM content on Young's modulus and tensile strength of the composite; (c) Stress-strain curves of PUT2-ZnO_2 composite after being reprocessed; (d) The relationship between tensile strength and elongation at break of the composite with 2 wt% ZnO-TPM and the number of reprocessing.

https://doi.org/10.1007/s10118-024-3121-9

the composites still showed the same decomposition stages as that of pure PUT matrix. The initial decomposition temperatures of the samples with ZnO-TPM contents of 0 wt%, 0.2 wt%, 0.5 wt%, 1 wt%, and 2 wt% are 241.8, 232.4, 224.9, 214.8, and 194.4 °C, respectively, which show a noteworthy decrease, suggesting that the thermal stability of PUT-based composites was reduced remarkably with more ZnO-TPM being incorporated. The maximum decomposition temperatures of these samples are 319.3, 317.7, 315.6, 317.5, and 320.2 °C, respectively, all with no much difference. The weight residues could be enlarged as more ZnO-TPM was used, those values are 0.53%, 1.79%, 2.00%, 2.07%, and 3.20% at ZnO-TPM content of 0, 0.2 wt%, 0.5 wt%, 1 wt% and 2 wt%, respectively. These results suggested that no evident effect on the decomposition stages of the composite was observed, whereas the thermal stability (*i.e.*, initial decomposition temperature) would be weakened obviously by ZnO-TPM. Our results herein are similar to that of the previous work, and this phenomenon might be attributed to the thermal catalysis of ZnO nanoparticles, which would accelerate the decomposition of the polymer matrix, decreasing thermal stability of the nanocomposites.[43] However, whether incorporating ZnO nanoparticles has an effect on the long-term stability of HUB in different environmental conditions needs to be studied further.

Fig. 10 shows the UV-Vis spectra of PUT2 sample and PUT-based composite (with thickness of ~150 μm). According to the spectrum of PUT2, it can be observed that the absorbance at 400-800 nm visible region was extremely weak and it would be strengthened remarkably at lower wavelength region, especially at 200–350 nm. Relative to the PUT2 sample, the composites would become increasingly opaque (Fig. S12 in ESI) and the absorbance of the composites was enhanced terribly with increasing the content of ZnO-TPM. That may result from the difference in refractive index between PUT matrix and ZnO-TPM, so more light scattering would occur in the composite with more ZnO-TPM. The conspicuous absorbance peaks at 375 nm, corresponding to the exciton state in the bulk ZnO,[44] was enhanced with increasing the ZnO-TPM content. For PUT2-ZnO_2 composite, the UV light at 200–400 nm could be absorbed efficiently. In this system, the modified ZnO nanoparticles are directly blended into the PUT liquid resin which can be applied to a variety of flat structures or items, then the resin can be quickly cured into a film under the action of UV light. It can be therefore expected that the PUT-based composites with ZnO-TPM can easily achieve UV-shielding in a low-cost and efficient manner. Especially, the combination of reprocessability and UV shielding property should make the composite potentially suitable as novel protective coating.

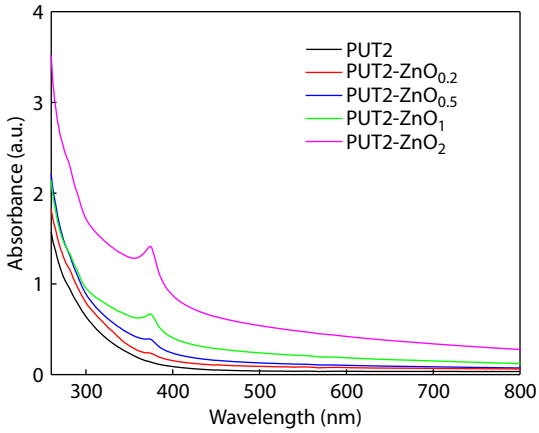

Fig. 10 UV-Vis spectra of PUT2 sample and the composites with different ZnO-TPM contents.

CONCLUSIONS

In this study, two kinds of prepolymers were prepared facilely *via* one-pot process, one using TBEM to form polyurethane-urea methacrylate prepolymer PUT bearing HUB motifs, another using HPMA to form ordinary polyurethane methacrylate prepolymer PUH. The structures of the prepolymers were confirmed by GPC, FTIR, and ^{1}H-NMR. Then, the thermosets were fabricated *via* UV curing of the prepolymers, and their thermal behavior and mechanical property were compared and discussed. Simply adjusting the feeding formula of the raw materials, the thermosets with changeable mechanical property could be fabricated. In comparison with PUH sample, PUT samples exhibited the features of solubility and recyclability under high temperature owing to the HUB motifs. Although the dynamic dissociation may occur in HUB, PUT samples manifested favorable solvent resistance and thermal stability at ambient temperature just like conventional thermosets. Besides, dynamic behavior of HUB was further approved by temperature-dependent FTIR and DMA. In addition, modified ZnO nanoparticles by silane coupling agent were incorporated into PUT to form their composite *via* UV curing. Results revealed that the Young's modulus and tensile strength of the composites increased gradually to the maximum values at 1 wt% ZnO-TPM content, and then decreased at 2 wt% content due to agglomeration. The composites also exhibited good reprocessability with improved recovery ratios in both elongation at break and ultimate tensile strength compared to pure PUT sample. However, ZnO-TPM would adversely reduce the initial decomposition temperature of the composites. The composite also had strong UV absorption capacity because of the incorporated ZnO-TPM. Considering the widely adjustable mechanical properties, the ability to be recycled for many times and high UV absorption capacity, the PUT-based composites with ZnO-TPM nanoparticles should hold great promise in serving as UV protective coating.

Conflict of Interests

The authors declare no interest conflict.

Electronic Supplementary Information

Electronic supplementary information (ESI) is available free of charge in the online version of this article at http://doi.org/10.1007/s10118-024-3121-9.

Data Availability Statement

The related data for this paper is confidential.

REFERENCES

1 Fortman, D. J.; Brutman, J. P.; De Hoe, G. X.; Snyder, R. L.; Dichtel, W. R.; Hillmyer, M. A. Approaches to sustainable and continually recyclable cross-linked polymers. *ACS Sustainable Chem. Eng.* **2018**, *6*, 11145–11159.
2 Lyu, M.; Liu, Y.; Yang, X.; Liang, D.; Wang, Y.; Liang, X.; Hu, Y.; Liang, L.; Zhang, C. Vanillin-based liquid crystalline polyimine thermosets and their composites for recyclable thermal management application. *Compos. Part B: Eng.* **2023**, *250*, 110462.
3 Zhao, X.; Long, Y.; Xu, S.; Liu, X.; Chen, L.; Wang, Y. Z. Recovery of epoxy thermosets and their composites. *Mater. Today* **2023**, *64*, 72–97.
4 Post, W.; Susa, A.; Blaauw, R.; Molenveld, K.; Knoop, R. J. I. A review on the potential and limitations of recyclable thermosets for structural applications. *Polym. Rev.* **2020**, *60*, 359–388.
5 Jehanno, C.; Sardon, H. A step towards truly recyclable plastics. *Nature* **2019**, *568*, 467–468.
6 Zou, W.; Dong, J.; Luo, Y.; Zhao, Q.; Xie, T. Dynamic covalent polymer networks: from old chemistry to modern day innovations. *Adv. Mater.* **2017**, *29*, 1606100.
7 Jin, Y.; Yu, C.; Denman, R. J.; Zhang, W. Recent advances in dynamic covalent chemistry. *Chem. Soc. Rev.* **2013**, *42*, 6634–6654.
8 Miao, W.; Yang, B.; Jin, B.; Ni, C.; Feng, H.; Xue, Y.; Zheng, N.; Zhao, Q.; Shen, Y.; Xie, T. An orthogonal dynamic covalent polymer network with distinctive topology transformations for shape- and molecular architecture reconfiguration. *Angew. Chem. Int. Edi.* **2022**, *61*, e202109941.
9 Lee, J.; Nanthananon, P.; Kim, A.; Kwon, Y. K. Malleable and recyclable thermoset network with reversible β-hydroxyl esters and disulfide bonds. *J. Appl. Polym. Sci.* **2023**, *140*, e53369.
10 Di Mauro, C.; Malburet, S.; Graillot, A.; Mija, A. Recyclable, repairable, and reshapable (3R) thermoset materials with shape memory properties from bio-based epoxidized vegetable oils. *ACS Appl. Bio Mater.* **2020**, *3*, 8094–8104.
11 Zhou, Q.; Fang, C.; Li, X.; You, L.; Qi, Y.; Liu, M.; Xu, Y.; He, Q.; Lu, S.; Zhou, Y. Room-temperature green recyclable epoxy composites with enhanced mechanical and thermal properties cross-linked *via* B-O-C bonds. *Chemistryselect* **2022**, *7*, e202200744.
12 Li, L.; Chen, X.; Jin, K.; Bin Rusayyis, M.; Torkelson, J. M. Arresting elevated-temperature creep and achieving full cross-link density recovery in reprocessable polymer networks and network composites *via* nitroxide-mediated dynamic chemistry. *Macromolecules* **2021**, *54*, 1452–1464.
13 Obadia, M. M.; Mudraboyina, B. P.; Serghei, A.; Montarnal, D.; Drockenmuller, E. Reprocessing and recycling of highly cross-linked ion-conducting networks through transalkylation exchanges of C-N bonds. *J. Am. Chem. Soc.* **2015**, *137*, 6078–6083.
14 Zhao, S.; Abu-Omar, M. M. Recyclable and malleable epoxy thermoset bearing aromatic imine bonds. *Macromolecules* **2018**, *51*, 9816–9824.
15 Zhu, G.; Zhang, J.; Huang, J.; Qiu, Y.; Liu, M.; Yu, J.; Liu, C.; Shang, Q.; Hu, Y.; Hu, L.; Zhou, Y. Recyclable and reprintable biobased photopolymers for digital light processing 3D printing. *Chem. Eng. J.* **2023**, *452*, 139401.
16 Jiang, L.; Lei, Y.; Xiao, Y.; Fu, X.; Kong, W.; Wang, Y.; Lei, J. Mechanically robust, exceptionally recyclable and shape memory cross-linked network based on reversible dynamic urea bonds. *J. Mater. Chem. A* **2020**, *8*, 22369–22378.
17 Ying, H.; Zhang, Y.; Cheng, J. Dynamic urea bond for the design of reversible and self-healing polymers. *Nat. Commun.* **2014**, *5*, 3218.
18 Zhang, Y.; Ying, H.; Hart, K. R.; Wu, Y.; Hsu, A. J.; Coppola, A. M.; Kim, T. A.; Yang, K.; Sottos, N. R.; White, S. R.; Cheng, J. Malleable and recyclable poly(urea-urethane) thermosets bearing hindered urea bonds. *Adv. Mater.* **2016**, *28*, 7646–7651.
19 Xie, S.; Wang, D.; Zhang, S.; Xu, J.; Fu, J. High performance poly(methyl methacrylate) *via* hindered urea bond crosslinking. *J. Mater. Chem. A* **2022**, *10*, 9753–9753.
20 Ren, S.; Zhou, W.; Song, K.; Gao, X.; Zhang, X.; Fang, H.; Li, X.; Ding, Y. Robust, self-healing, anti-corrosive waterborne polyurethane urea composite coatings enabled by dynamic hindered urea bonds. *Prog. Org. Coat.* **2023**, *180*, 107571.
21 Lu, X.; Zhang, L.; Zhang, J.; Wang, C.; Zhang, A. Facile preparation of dual functional wearable devices based on hindered urea bond-integrated reprocessable polyurea and agnws. *ACS Appl. Mater. Interfaces* **2022**, *14*, 41421–41432.
22 Zhou, Z.; Wang, X.; Yu, H.; Yu, C.; Zhang, F. Dynamic cross-linked polyurea/polydopamine nanocomposites for photoresponsive self-healing and photoactuation. *Macromolecules* **2022**, *55*, 2193–2201.
23 Banitaba, S. N.; Semnani, D.; Heydari-Soureshjani, E.; Ul Arifeen, W.; Ko, T. J.; Rezaei, B.; Ensafi, A. A.; Latifi, M.; Mostafavi, E.; Kaushik, A. K. Nanocomposite with fast Li^+ ion conductivity: a solvent-free polymer electrolyte reinforced with decorated Fe_3O_4 nanoparticles. *ACS Appl. Energy Mater.* **2023**, *6*, 4704–4714.
24 Gniadek, M.; Krolikowska, A.; Malinowska, S.; Donten, M. Influence of nanostructural additives on the properties of polypyrrole-based composites. *Electroanal. Chem.* **2023**, *938*, 117409.
25 Alshoaibi, A. Dyes confinement in the nano scale and converting poly vinyl alcohol to be optical-active polymeric nanocomposites with high thermal stability. *Polymers* **2023**, *15*, 2310.
26 Cazan, C.; Enesca, A.; Andronic, L. Synergic effect of TiO_2 filler on the mechanical properties of polymer nanocomposites. *Polymers* **2021**, *13*, 2017.
27 Rahman, M. M. Polyurethane/zinc oxide (PU/ZnO) composite-synthesis, protective property and application. *Polymers* **2020**, *12*, 1535.
28 Pushpalatha, C.; Suresh, J.; Gayathri, V. S.; Sowmya, S. V.; Augustine, D.; Alamoudi, A.; Zidane, B.; Albar, N. H. M.; Patil, S. Zinc oxide nanoparticles: a review on its applications in dentistry. *Front. Bioeng. Biotech.* **2022**, *10*, 917990.
29 Abu Hanif, M.; Kim, Y. S.; Akter, J.; Kim, H. G.; Kwac, L. K. Fabrication of robust and stable N-doped ZnO/single-walled carbon nanotubes: characterization, photocatalytic application, kinetics, degradation products, and toxicity analysis. *ACS Omega* **2023**, *8*, 16174–16185.
30 Bharti; Jangwan, J. S.; Kumar, S. S.; Kumar, V.; Kumar, A.; Kumar, D. A review on the capability of zinc oxide and iron oxides nanomaterials, as a water decontaminating agent: adsorption and photocatalysis. *Appl. Water Sci.* **2022**, *12*, 46.
31 Tang, J. F.; Fang, C. C.; Hsu, C. L. Enhanced organic gas sensor based on cerium- and Au-doped ZnO nanowires *via* low temperature one-pot synthesis. *Appl. Surf. Sci.* **2023**, *613*, 156094.
32 Bhadwal, N.; Ben Mrad, R.; Behdinan, K. Review of zinc oxide piezoelectric nanogenerators: piezoelectric properties, composite structures and power output. *Sensors* **2023**, *23*, 3859.
33 Cui, X.; Wang, L.; Dong, Q.; Liang, W.; Zhao, S. Synthesis and characterization of a UV-resistant ZnO/pyrophyllite nanocomposite prepared by solid-state reaction method. *Ceram. Int.* **2022**, *48*, 34084–34091.
34 Lizundia, E.; Ruiz-Rubio, L.; Luis Vilas, J.; Manuel Leon, L. Poly(L-lactide)/ZnO nanocomposites as efficient UV-shielding coatings for packaging applications. *J. Appl. Polym. Sci.* **2016**, *133*, 42426.
35 Zhao, Z.; Mao, A.; Gao, W.; Bai, H. A facile *in situ* method to fabricate transparent, flexible polyvinyl alcohol/ZnO film for UV-shielding. *Compos. Commun.* **2018**, *10*, 157–162.
36 Zhou, J.; Tang, L. Synthesis and structure of 2-hydroxypropyl

methacrylate-capped isophorone diisocyanate and poly(propylene glycol) urethane mixtures and the properties of their UV-cured co-networks with isobornyl methacrylate. *Materials* **2022**, *15*, 8586.
37 Zhou, Z.; Chen, S.; Xu, X.; Chen, Y.; Xu, L.; Zeng, Y.; Zhang, F. Room temperature self-healing crosslinked elastomer constructed by dynamic urea bond and hydrogen bond. *Prog. Org. Coat.* **2021**, *154*, 106213.
38 Xie, D. M.; Zhang, Y. X.; Li, Y. D.; Weng, Y.; Zeng, J. B. Castor oil-derived sustainable poly(urethane urea) covalent adaptable networks with tunable mechanical properties and multiple recyclability based on reversible piperidine-urea bond. *Chem. Eng. J.* **2022**, *446*, 137071.
39 Zhang, J.; Zhang, C.; Shang, Q.; Hu, Y.; Song, F.; Jia, P.; Zhu, G.; Huang, J.; Liu, C.; Hu, L.; Zhou, Y. Mechanically robust, healable, shape memory, and reprocessable biobased polymers based on dynamic pyrazole-urea bonds. *Eur. Polym. J.* **2022**, *169*, 111133.
40 Wu, Q.; Hu, Y.; Tang, J.; Zhang, J.; Wang, C.; Shang, Q.; Feng, G.; Liu, C.; Zhou, Y.; Lei, W. High-performance soybean-oil-based epoxy acrylate resins: "Green" synthesis and application in UV-curable coatings. *ACS Sustainable Chem. Eng.* **2018**, *6*, 8340–8349.
41 Li, T.; Xie, Z.; Xu, J.; Weng, Y.; Guo, B. H. Design of a self-healing cross-linked polyurea with dynamic cross-links based on disulfide bonds and hydrogen bonding. *Eur. Polym. J.* **2018**, *107*, 249–257.
42 Bin Rusayyis, M. A.; Torkelson, J. M. Reprocessable and recyclable chain-growth polymer networks based on dynamic hindered urea bonds. *ACS Macro Lett.* **2022**, *11*, 568–574.
43 Ma, X. Y.; Zhang, W. D. Effects of flower-like ZnO nanowhiskers on the mechanical, thermal and antibacterial properties of waterborne polyurethane. *Polym. Degrad. Stabil.* **2009**, *94*, 1103–1109.
44 Kim, D.; Jeon, K.; Lee, Y.; Seo, J.; Seo, K.; Han, H.; Khan, S. Preparation and characterization of UV-cured polyurethane acrylate/ZnO nanocomposite films based on surface modified zno. *Prog. Org. Coat.* **2012**, *74*, 435–442.

https://doi.org/10.1007/s10118-024-3121-9